DOI: 10.1002/ejic.200600850

Synthesis of Controllable-Size Core–Shell Se@Ag and Se@Au Nanoparticles in UV-Irradiated TSA Solution

Liangbao Yang,[a] Yuhua Shen,*[a,b] Anjian Xie,[a,b] Jianjun Liang,[a] Jinmiao Zhu,[a] and Long Chen[a]

Keywords: Nanostructures / Photochemistry / Core–shell structures / Selenium

The formation of Se-core–Au-shell and Se-core–Ag-shell nanoparticles by using photochemically reduced tungstosilicate Keggin ions has been described. The Se core structure serves both as a chemical and a physical template for the coating of Au and Ag. With this method, the core size and the shell thickness can be controlled by varying the conditions. With this strategy, it is possible to realize a large combination of core–shell nanostructures with potential application in engineered nanomaterials and catalysis by using Keggin ions.

(© Wiley-VCH Verlag GmbH & Co. KGaA, 69451 Weinheim, Germany, 2007)

Introduction

For many years, considerable effort has been made to design, fabricate and manipulate nanostructured systems with functional properties.[1] This knowledge, together with effective strategies towards the fabrication of nanostructures, has inspired the design and development of new composites for advanced applications. Core–shell structures provide a useful means to modify the properties of nanoparticles.[2] Such core–shell nanoparticles have become attractive because of the advantages offered by the combination of the properties of different compositions and of the shelled structures. They are used as building blocks for photonic crystals,[3] as heterogeneous catalysts,[4] in multienzyme biocatalysis,[5] and in surface-enhanced Raman scattering[6] and drug-delivery applications.[7] Most studies on the core–shell particles have focused on composites that are typically composed of solid or liquid cores surrounded by shells of polymers, inorganic compounds, or biomacromolecules. They provide the possibility of enhanced functionality and multifunctional properties, which is in contrast with their more-limited, single-component counterparts.

Semiconductor-metal core–shell structures are most interesting because of the bifunctional properties of the metal and the semiconductor.[8–10] In this work, we report a facile, one-pot synthesis of Se@Au and Se@Ag composite colloids in UV-irradiated TSA solution. Such Se@Au(Ag) nanocomposite colloids are expected to be useful in biotechnology, as Se is an essential trace element for humans. Further, Se is an important elemental semiconductor, because of its many intriguing photoelectrical properties as well as its applications in semiconductor rectifiers, solar cells, photographic exposure meters, and xerography.[11] Silver or gold exhibits high-temperature and high-pressure stability and resistance to acids, bases, and solvents.[12] Combination of the two nanomaterials of Se and Au or of Se and Ag provides a model structure for the further understanding of the core–shell heterostructures and their properties. The composite colloids produced are also expected to have potential applications in electronics, photonics, catalysis, and sensors. Metal-based materials with nanoscale hollow interiors exhibit promising properties for diverse applications.[13] As reported previously,[14] the Se-core composites can be used as precursors to yield hollow capsules by subsequent removal of the sacrificial Se cores; this is because Se exhibits high solubility in various solvents (e.g. CS_2 and N_2H_4) and a relatively low melting point (≈ 217 °C).[11]

Experimental procedures for the synthesis of core–shell nanostructures are rather cumbersome and involve several steps. Generally, growth of core–shell structures can be accomplished by the successive reduction of one metal ion over the core of another.[15–18] Keggin ions have a special structure, which may be reduced photochemically.[19,20] Sastry and co-workers have demonstrated that bimetallic nanoparticles can be synthesized by using Keggin ions as a UV-switchable reducing agent.[21,22] In this paper, we use a strategy that involves the immobilization of a reducing agent such as tungstosilicate acid (TSA) in the solution of the core, which, when exposed to the second metal ions, can selectively reduce them on the surface to lead to phase-pure

[a] School of Chemistry and Chemical Engineering, Anhui University,
Hefei 230039, P. R. China
Fax: +86-551-5107342
E-mail: s_yuhua@163.com
[b] State Key Laboratory of Coordination Chemistry, Nanjing University,
Nanjing 210093, P. R. China
[c] Chuzhou Vocational Technology College,
Chuzhou 239000, P. R. China

 © 2007 Wiley-VCH Verlag GmbH & Co. KGaA, Weinheim

core–shell structures. An advantageous feature of this approach for obtaining phase-pure core–shell nanoparticle structures could be a reducing agent bound to the surface of the core nanoparticle that can be selectively activated (i.e. whose reducing capability can be switched off and on at will). The mechanism is also discussed. Presented below are details of the investigation.

Results and Discussion

Figures 1A and B show the UV/Vis spectra of the Se-core–Au-shell and Se-core–Ag-shell nanoparticle solutions, respectively, at different stages of preparation. Curve 1 in Figure 1 corresponds to the spectrum of a 1 mM TSA/1 mM H_2SeO_3 aqueous solution. It can be observed that there is no absorption in the visible region of the electromagnetic spectrum. The UV/Vis absorption spectrum recorded after UV irradiation of the TSA/H_2SeO_3 solution for 5 h is shown as curve 2 in Figure 1. It can be clearly seen that an absorption band starts to form from ca. 655 nm. This absorption band may arise as a result of excitation of the surface plasmon vibrations in the Se nanoparticles.[23] The TSA/Se nanoparticle solution was further irradiated with UV light for 3 h; this UV/Vis spectrum is shown as curve 3 in Figure 1. At this stage, the color of the solution changed from orange to bluish-red; these changes are reflected as an increase in absorption at 760 nm in the spectrum. This increase in absorption at long wavelengths clearly indicates that the TSA ions have been reduced.[20] Curve 4 in Figure 1 corresponds to the UV/Vis spectra of the UV-irradiated TSA/Se nanoparticle solution after addition of $HAuCl_4$ (Figure 1A) and $AgNO_3$ solutions (Figure 1B). Strong absorption bands at ca. 540 nm and ca.410 nm are observed. These absorption bands arise from excitation of the surface plasmon vibrations in the Au[20,21,24] and Ag[20,21] nanoparticles. Curve 5 in Figure 1 corresponds to the TSA/Se solution without further UV irradiation (sample 2) with the addition of 10^{-3} M aqueous solutions of $HAuCl_4$ (Figure 1A) and $AgNO_3$ (Figure 1B). When curves 4 and 5 in Figures 1A and B are compared, large changes in both the UV/Vis absorption spectra of the gold and silver nanoparticle solutions are observed. Thus, the photochemical charging of the TSA molecules is the most crucial step in the protocol, which sets this protocol apart from other bimetallic nanoparticle core–shell synthesis protocols that employ reducing agents present uniformly in the reaction media. That the reducing capability of the TSA ions can be switched on by irradiation with UV light is an additional feature that enhances the versatility of this technique.

The XRD pattern recorded from a drop-coated film of the UV-irradiated TSA solution after addition of H_2SeO_3 on a glass substrate is shown in Figure 2, curve 1. All of the strong and sharp reflection peaks can readily be indexed to a single phase of trigonal-structured selenium (indicated by "*", JCPDS Cards No. 86-2246). Curve 2 in Figure 2 shows the XRD pattern recorded from a drop-coated film of the UV-irradiated TSA/Se solution after addition of $HAuCl_4$ (Figure 2A) and $AgNO_3$ (Figure 2B) solutions. The (111), (200), and (220) Bragg reflections of face-centered cubic gold and silver are clearly observed. The background is most likely caused by Brownian motion of the particles during the scan, solvent scattering, or the short-range order of the solvation cage around the particles. The results, obtained from XRD, indicate that the products of Se and Au/Ag are crystalline and have a high purity.

To confirm the presence of Se, Au, and Ag in Se–Au- and Se–Ag-core–shell nanoparticles, a chemical analysis of these samples was performed by using XPS. The Se 3d core level spectra recorded from the Se-core–Au-shell and Se-core–Ag-shell nanoparticles at various stages of preparation are shown in Figure 3A and Figure 3B, respectively, while the Au 4f core level spectrum from the Se-core–Au-shell sample and the Ag 3d core level spectrum from the Se-core–Ag-shell nanoparticles are shown in Figure 3C and Figure 3D, respectively. The binding energy at 53.61 eV (Figure 3A) or 54.32eV (Figure 3B), corresponding to Se 3d, is the characteristic peak for elemental selenium,[25,26] which

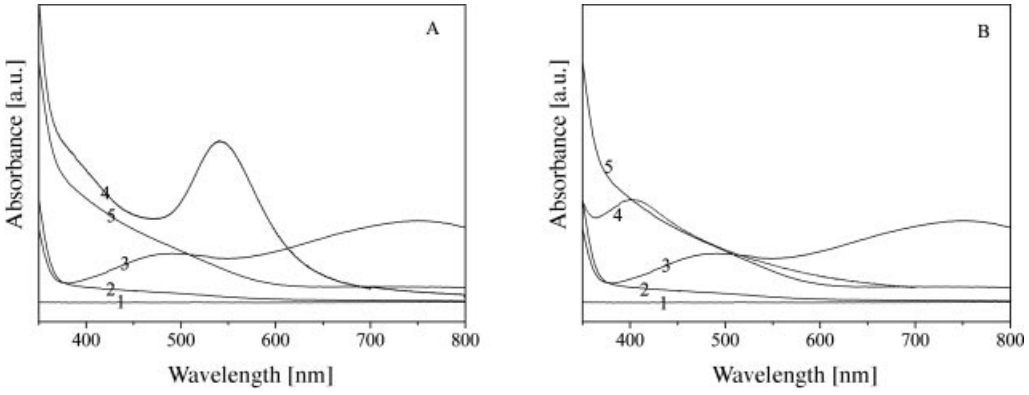

Figure 1. (A) and (B) show the UV/Vis spectra of the Se-core–Au/Ag-shell nanoparticle solutions at different stages of reaction. Curve 1 in (A) and (B): 10^{-3} M TSA/10^{-3} M H_2SeO_3 aqueous solution before UV irradiation; curve 2 in (A) and (B): TSA/H_2SeO_3 solution (sample 1) after UV irradiation for 5 h.; curve 3 in (A) and (B): further UV irradiation of sample 2 (for 3 h); curve 4: addition of 10^{-3} M $HAuCl_4$ (A) and $AgNO_3$ (B) solutions to sample 3; curve 5: addition of 10^{-3} M aqueous solutions of $HAuCl_4$ (A) and $AgNO_3$ (B) to sample 2 (no further UV irradiation).

 © 2007 Wiley-VCH Verlag GmbH & Co. KGaA, Weinheim

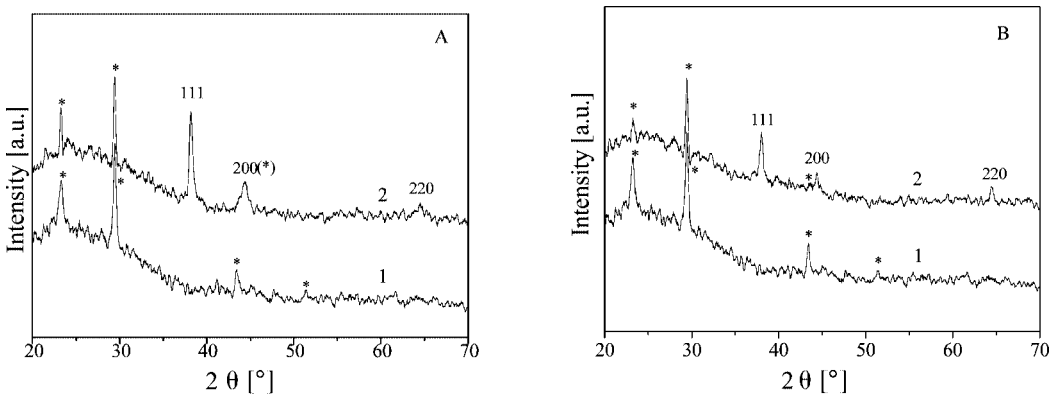

Figure 2. (A) and (B) show the XRD patterns recorded from drop-coated films on glass substrates of the Se-core–Au/Ag-shell nanoparticle solutions at different stages of reaction. Curve 1 in (A) and (B): UV-irradiated TSA solution after addition of 10^{-3} M H_2SeO_3; Curve 2: UV-irradiated TSA/Se solution after addition of 10^{-3} M $HAuCl_4$ (A) and $AgNO_3$ (B) solutions. The Bragg reflections marked * correspond to Se.

implies that the valence of selenium in the core is zero. The Au 4f core level spectrum recorded from the Se–Au-core–shell nanoparticle sample could be resolved into a single spin-orbit pair (spin-orbit splitting ≈ 3.71 eV) with a $4f_{7/2}$ binding energy (BE) of 83.68 eV (Figure 3C). This BE is characteristic of Au in the fully reduced state.[27] The Ag 3d spectrum (Figure 3D) resolves into two spin-orbit components. The Ag $3d_{5/2}$ and $3d_{3/2}$ peaks occur at a BE of 367.8 and 373.8 eV, respectively, and correspond to metallic silver.[28] This result demonstrates that only one form of Ag is present in solution, in the form of Ag^0.

Figure 4 shows a representative TEM image of the Se nanoparticle solution. From the TEM image, it can clearly be seen that the nanoparticles, with an average size in diameter of 40 nm, are spherical colloids. Figure 5A and Figure 6A display the SEM images of Se@Au- and Se@Ag-

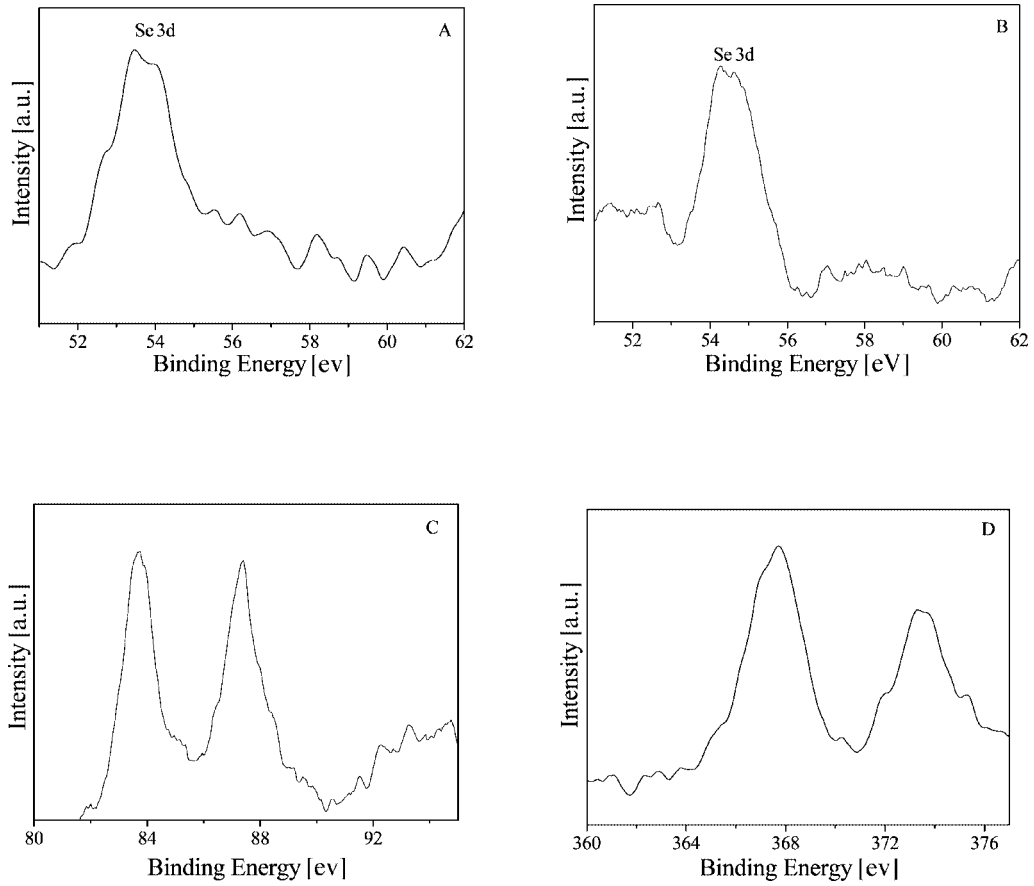

Figure 3. Se 3d core level spectra recorded from Se–Au- (A) and Se–Ag-core–shell nanoparticles (B). Au 4f (C) and Ag 3d (D) core level spectrum recorded from Se–Au- and Se–Ag-core–shell nanoparticles, respectively.

 © 2007 Wiley-VCH Verlag GmbH & Co. KGaA, Weinheim

core–shell colloids formed by sequential reduction by a UV-irradiated TSA solution. Such core–shell colloids were quite uniform and could be obtained in copious quantities. Figure 5B and Figure 6B show the TEM images of the same samples of Figure 5A and Figure 6A, respectively, which reveal the smoothness and uniformity of these spheres with sizes in diameter of 51 nm and 99 nm, respectively. Again, the Se cores could selectively be removed by chemical or thermal means.[14] When the Se@Au and Se@Ag nanoparticles (Figures 5A,B and 6A,B) are compared with the Se nanoparticles (Figure 4), it can be seen that the particles are quite monodisperse and show a small increase in size (ranging from 40 nm to 51 nm and to 99 nm, respectively).

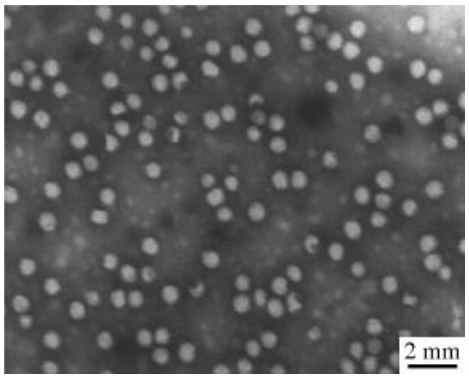

Figure 4. TEM image of Se nanoparticles reduced by UV-irradiated TSA solution.

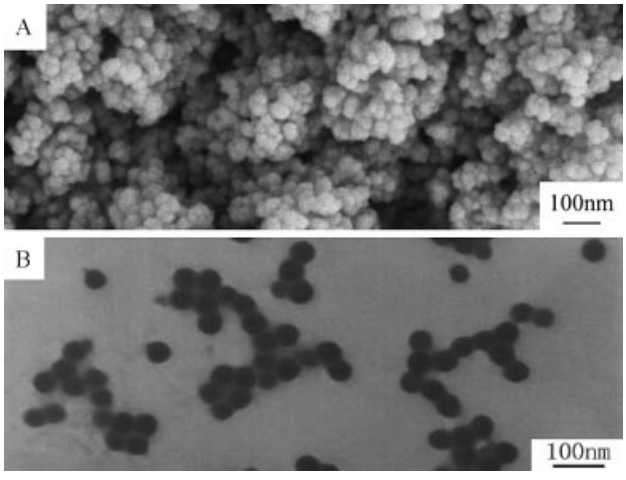

Figure 5. (A) SEM of Se@Au-core–shell colloids formed by sequential reduction of selenium and gold ions by UV-irradiated TSA solution. (B) TEM of the same sample.

Figure 7 shows the TEM image of Au nanoparticles reduced by a UV-irradiated TSA solution. From Figure 7, it can clearly be seen that the gold nanoparticles are very different from those covering the templates of Se. This control experiment thus clearly shows that the template in the nucleation step facilitates the formation of the coating on the template. From Figures 5 and 6, we notice that the t-Se templates are well coated by the Au and Ag nanoshells. In our study, we believe that the Se structures serve as both chemical and physical templates.[14a] The coating of Se templates

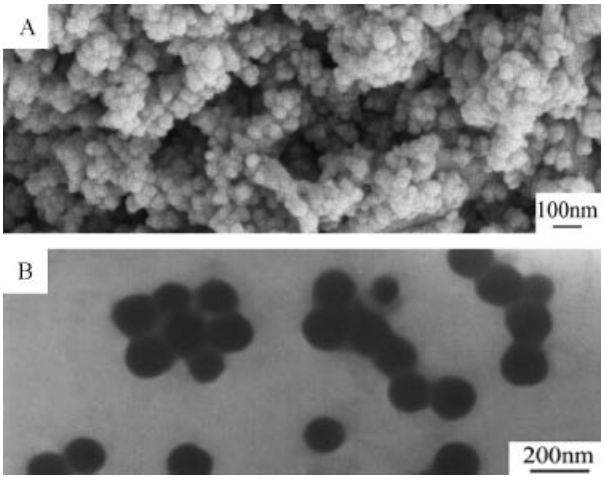

Figure 6. (A) SEM of Se@Ag-core–shell colloids formed by sequential reduction of selenium and gold ions by UV-irradiated TSA solution. (B) TEM of the same sample.

with Au and Ag is believed to occur through two distinct reduction reactions: (i) the initial reduction of the Au^{III} or Ag^{I} salt by the Se template itself at the interface, which is similar to the method described in the literature[29], and (ii) the reduction of the Au^{III} or Ag^{I} salt by the UV-irradiated TSA solution. The galvanic reduction of Au^{III} or Ag^{I} by a Se template can continue until the surface is completely covered. Subsequent deposition of the Au- or Ag coating is dominated by the UV-irradiated TSA solution. The engagement of the template in the nucleation step facilitates the formation of homogeneous, uniform coating on the template. This is also the major reason why Se is such a good template for the coating by metals relative to inert structures such as polystyrene beads or silica spheres. On the other hand, we believe that such spontaneous "landing" of the small nanoparticles of Au or Ag on the backbone of the Se nanoparticles followed by self aggregation rather than aggregation with the Se nanoparticles can be related to the "contact epitaxy" mechanism proposed by Averback et al.[30,31] The driving force for this spontaneous, oriented attachment is substantial reduction in the surface free energy (from a thermodynamic viewpoint) that arises as a result of the elimination of pairs of high energy surfaces.[32,33] The

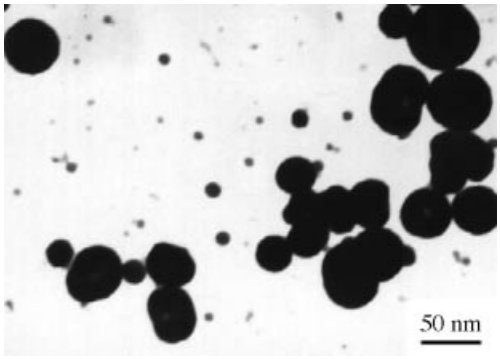

Figure 7. TEM image of Au nanoparticles reduced by UV-irradiated TSA solution.

 © 2007 Wiley-VCH Verlag GmbH & Co. KGaA, Weinheim

initial randomly oriented nanocrystals can align epitaxially with the substrate (the Se nanoparticles in this case), which can be explained by the rotation of the nanoparticles within the aggregates that is driven by short-range interactions between adjacent surfaces.[30,31]

Figures 8A and B show the dependence of the diameters of the Se–Au- and Se–Ag-core–shell nanoparticles, respectively, on pH. In Figure 8 a, b, c, and d four samples with pH of 1.5, 2.5, 3.5, and 4.5, respectively, are represented. In Figure 8A, the mean diameters of the four samples of the Se-core–Au-shell are 59.5 nm, 51.1 nm, 48 nm, and 47.4 nm, respectively. From Figure 8A, it can clearly be seen that the diameter of the particles continuously decreases with increasing pH from 1.5 to 4.5. However, the rate at which the diameter decreases diminishes gradually, and when the pH is >4, the decrease in the diameter of the Se-core–Au-shell nanoparticles is minimal. In Figure 8B, the mean diameters of the four samples of the Se-core–Ag-shell are 95.6 nm, 99.3 nm, 125.5 nm, and 128 nm. From Figure 8B, it can clearly be seen that the diameter of the particles continuously increases with increasing pH from 1.5 to 4.5. In the regions between 1.5 and 2.5 and between 3.5 and 4.5, the increase in the diameter of the Se-core–Ag-shell nanoparticles is slight; however, there is a great increase in the region between pH 2.5 and 3.5. Comparing Figures 8A and B, we notice that the diameter of the Se-core–Au-shell nanoparticles decreases with increasing pH, while that of the Se-core–Ag-shell nanoparticles increases.

We also study the relationship between the diameter of the core shell nanoparticles and temperature, which is shown in Figures 9A (Se–Au) and B (Se–Ag). In Figure 9 a, b, c, and d four samples the- core–shell nanoparticles having different diameters at 20, 40, 60, and 80 °C, respectively, are represented. The mean diameters of the four typical samples of the Se-core–Au-shell are 52.3 nm, 60.3 nm, 66.3 nm, and 69.1 nm, respectively. As demonstrated in Figure 9A, the size of these colloids can conveniently be controlled by simply varying the reaction temperature, i.e. the diameter continuously increases with an increase in the temperature. In Figure 9B, the mean diameters of the four samples of the Se-core–Ag-shell are 105 nm, 99 nm, 69.2 nm, and 47.2 nm. It can clearly be seen from Figures 9A and B that the diameter of Se-core–Au-shell nanoparticles increases with increasing temperature, while that of Se-core–Ag-shell nanoparticles decreases. The reasons for the above phenomena are not clear yet.

Since the size of these core–shell nanoparticles can conveniently be controlled by simply varying the pH of the reaction solution and the reaction temperatures, it is believed that the procedure described here should provide an effective route to produce Se@Au and Se@Ag nanoparticles with controllable size. In this current investigation in which

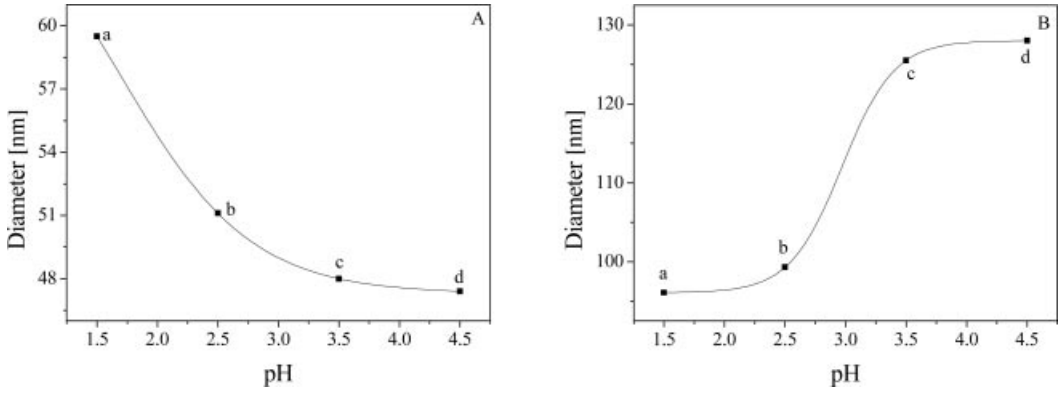

Figure 8. (The dependence of the diameter of the Se–Au- (A) and Se–Ag-core–shell nanoparticles (B) on pH. a, b, c, and d correspond to a pH value of 1.5, 2.5, 3.5, and 4.5, respectively. (Conditions: temperature, ca. 25 °C; the diameter of the Se core, ca.40 nm).

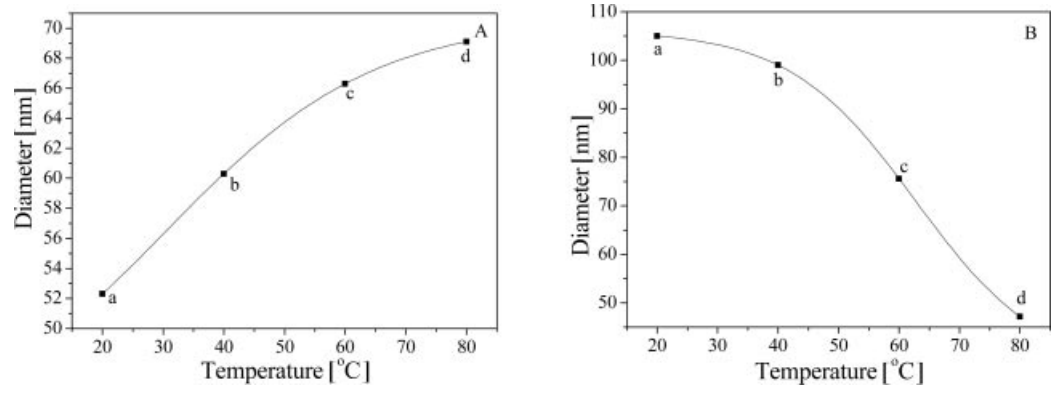

Figure 9. The dependence of the diameter of the Se–Au- (A) and Se–Ag-core–shell nanoparticles (B) on temperature. a, b, c, and d correspond to 20, 40, 60, and 80 °C. (Conditions: pH, ca. 2.5; the diameter of the Se core, ca.40 nm).

 © 2007 Wiley-VCH Verlag GmbH & Co. KGaA, Weinheim

we studied the formation of the nanoparticles as a function of temperature, the size of the t-Se colloids could conveniently be controlled by simply varying the reaction temperature, which ranged from 20 to 80 °C; the diameter increased from about 44.7 to about 83.3 nm. We can therefore control the size of the core and the thickness of the shell. In principle, this procedure can be extended to several other noble metal shells that have been prepared as nanocomplexes by reduction with TSA-ion particles.

Conclusions

In summary, we have demonstrated the use of t-Se colloids as templates in forming controllable-size Se-core–Au/Ag-shell nanoparticle structures. It is also worth mentioning that the Se templates are not limited to the randomly dispersed nanostructures shown in this work. It has been demonstrated that the Se nanowires and colloids could be organized into ordered structures such as networks (or meshes) and crystalline lattices.[34] These templates are expected to play an increasingly important role in fabricating metal nanostructures with complex (yet controllable) morphologies. In addition, the monodisperse shells of Au/Ag will be suitable as a new class of building blocks to fabricate colloidal crystals that are expected to exhibit improved photonic bandgap properties.[35]

Experimental Section

Tungstosilicate acid [$H_4(SiW_{12}O_{40})$, TSA], selenious acid (H_2SeO_3), silver nitrate ($AgNO_3$), chloroauric acid ($HAuCl_4$), and 2-propanol [$CH_3CH(OH)CH_3$] were all A.R. grade and obtained from Shanghai reagent Co. All the reagents in the experiment were used as received. Doubly distilled water was used throughout to prepare the solutions.

In a typical experiment, an aqueous, deaerated solution of tungstosilicate acid (30 mL of a 1 mM solution), an aqueous, deaerated solution of H_2SeO_3 (30 mL of a 1 mM solution), and propan-2-ol (2 mL) were placed in a test tube. This mixture was irradiated with UV light (Pyrex filter, >280 nm, 450 W Hanovia medium pressure lamp) for 5 h. UV irradiation leads to the in situ reduction of H_2SeO_3 by the electron-rich $[SiW_{12}O_{40}]^{5-}$ ions {formed by the photochemical reduction of $[SiW_{12}O_{40}]^{4-}$ ions}, which can clearly be seen by the appearance of an orange solution. The above solution was further irradiated with UV light for 3 h, and the color of the solution changed from orange to bluish-red. To this solution (15 mL) were added aqueous solutions of $HAuCl_4$ and $AgNO_3$ (15 mL of 1 mM solution, each) separately whilst stirring. The color of the solutions changed from bluish-red to pink and light brown, which indicates the formation of gold and silver nanoparticles, respectively.

UV/Vis spectroscopic measurements of the samples were carried out with a TU-1901 model UV/Vis double beam spectrophotometer (Beijing Purkinje General Instrument Co., Ltd, China) operated at a resolution of 2 nm. XRD analyses of drop-coated films of the Se solution and Se@Ag and Se@Au on glass substrates were carried out with a MAP18AHF instrument (Japan MAC Science Co.). XPS measurements of the Se nanoparticles were carried out with a VG ESCALAB MKII instrument at a pressure $>10^{-6}$ Pa. The general scan and Se core-level spectra were recorded with non-monochromatized Mg–K_α radiation (photon energy = 1253.6 eV). The core-level binding energies (BEs) were aligned with respect to the C_{1s} BE of 285 eV. Samples for TEM analysis were prepared by drop-coating films of the Se solution and Se@Ag and Se@Au solutions on carbon-coated copper TEM grids and allowing the grid to stand for 2 min following which the extra solution was removed using blotting paper. The above TEM analysis was carried out with a JEM model 100SX electron microscope instrument (Japan Electron Co.) operated at an accelerating voltage at 80 kV. SEM measurements were carried out with a Leica Stereoscan-440 instrument equipped with a Phoenix energy dispersive analysis of X-rays (EDAX) attachment. The size distribution of the nanoparticles was measured by PCS on the Zetasizer $3000HS_A$ instrument (Malvern Instruments Limited).

Acknowledgments

This work is supported by the National Science Foundation of China (20471001, 20371001), the Specific Project for Talents of Science and Technology of Universities of Anhui Province (2005hbz03), the Key Laboratory of Environment-friendly Polymer Materials of Anhui Province, and Science Foundation of Anhui Province (2006KJ155B).

[1] a) Y. W. Cao, R. Jin, C. A. Mirkin, *J. Am. Chem. Soc.* **2001**, *123*, 7961–7962; b) W. Schartl, *Adv. Mater.* **2000**, *12*, 1899–1908; c) L. X. Cao, J. H. Zhang, S. L. Ren, S. H. Huang, *Appl. Phys. Lett.* **2002**, *80*, 4300–4302; d) J. C. Yu, X. C. Wang, L. Wu, W. K. Ho, L. Z. Zhang, G. T. Zhou, *Adv. Funct. Mater.* **2004**, *14*, 1178–1183; e) X. C. Wang, J. C. Yu, H. Y. Yip, L. Wu, P. K. Wang, S. Y. Lai, *Chem. Eur. J.* **2005**, *11*, 2997–3004; f) Y. J. Kang, T. A. Taton, *Angew. Chem.* **2005**, *117*, 413–416; *Angew. Chem. Int. Ed.* **2005**, *44*, 409–412.

[2] a) X. G. Peng, M. C. Schlamp, A. V. Kadavanich, A. P. Alivisatos, *J. Am. Chem. Soc.* **1997**, *119*, 7019–7029; b) S. U. Son, Y. Jang, J. Park, H. B. Na, H. M. Park, H. J. Yun, J. Lee, T. Hyeon, *J. Am. Chem. Soc.* **2004**, *126*, 5026–5027; c) X. W. Teng, D. Black, N. J. Watkins, Y. L. Gao, H. Yang, *Nano Lett.* **2003**, *3*, 261–264; d) H. Zeng, J. Li, Z. L. Wang, J. P. Liu, S. H. Sun, *Nano Lett.* **2004**, *4*, 187–190.

[3] A. Rogach, A. Susha, F. Caruso, G. Sukhorukov, A. Kornowski, S. Kershaw, H. Mohwald, A. Eychmuller, H. Weller, *Adv. Mater.* **2000**, *12*, 333–337.

[4] a) C. W. Chen, M. Q. Chen, T. Serizawa, M. Akashi, *Chem. Commun.* **1998**, 831–832; b) C. W. Chen, T. Serizawa, M. Akashi, *Chem. Mater.* **1999**, *11*, 1381–1389.

[5] a) C. Schuler, F. Caruso, *Macromol. Rapid Commun.* **2000**, *21*, 750–753; b) F. Caruso, H. Fiedler, K. Haage, *Colloids Surf. A* **2000**, *169*, 287–293.

[6] S. J. Oldenburg, S. L. Westcott, R. D. Averitt, N. J. Halas, *J. Chem. Phys.* **1999**, *111*, 4729–4739.

[7] a) K. S. Oh, K. E. Lee, S. S. Han, S. U. H. Cho, D. Kim, S. H. Yuk, *Biomacromolecules* **2005**, *6*, 1062–1067; b) K. S. Soppimath, D. C. W. Tan, Y. Y. Yang, *Adv. Mater.* **2005**, *17*, 318–323; c) T. Riley, C. R. Heald, S. Stolnik, M. C. Garnett, L. Illum, S. S. Davis, S. M. King, R. K. Heenan, S. C. Purkiss, R. J. Barlow, P. R. Gellert, C. Washington, *Langmuir* **2003**, *19*, 8428–8435.

[8] P. V. Kamat, B. Shanghavi, *J. Phys. Chem. B* **1997**, *101*, 7675–7679.

[9] I. Honma, T. Sano, H. Komiyama, *J. Phys. Chem.* **1993**, *97*, 6692–6695.

[10] Y. Lu, Y. D. Yin, Z. Y. Li, Y. A. Xia, *Nano Lett.* **2002**, *2*, 785–788.

[11] a) L. I. Berger, *Semiconductor Materials*, CRC, Boca Raton, FL, **1997**; b) D. M. Chizhikov, V. P. Schastlivy, *Selenium and*

 © 2007 Wiley-VCH Verlag GmbH & Co. KGaA, Weinheim

Selenides, Collet's, London, Wellingborough, **1968**; c) R. A. Zingaro, W. C. Cooper, *Selenium*, Van Nostrand Reinhold, New York, **1974**.
[12] A. H. Lu, W. C. Li, N. Matoussevitch, B. Spliethoff, H. Bonnemann, F. Schuth, *Chem. Commun.* **2005**, 98–100.
[13] a) G. S. Chai, S. B. Yoon, J. H. Kim, J. S. Yu, *Chem. Commun.* **2004**, 2766–2767; b) S. Han, Y. Yun, K. W. Park, Y. E. Sung, T. Hyeon, *Adv. Mater.* **2003**, *15*, 1922–1925; c) Y. D. Xia, R. Mokaya, *Adv. Mater.* **2004**, *16*, 886–891.
[14] a) B. Mayer, X. C. Jiang, D. Sunderland, B. Cattle, Y. N. Xia, *J. Am. Chem. Soc.* **2003**, *125*, 13364–13365; b) U. Y. Jeong, Y. N. Xia, *Adv. Mater.* **2005**, *17*, 102–106; c) X. C. Jiang, B. Mayers, Y. L. Wang, B. Cattle, Y. N. Xia, *Chem. Phys. Lett.* **2004**, *385*, 472–476.
[15] G. Schmid, A. Lehnert, J.-O. Malm, J.-O. Bovin, *Angew. Chem. Int. Ed. Engl.* **1991**, *30*, 874–876.
[16] X. Teng, D. Black, N. J. Watkins, Y. Gao, H. Yang, *Nano Lett.* **2003**, *3*, 261–264.
[17] C. S. Ah, S. D. Hong, D. J. Jang, *J. Phys. Chem. B* **2001**, *105*, 7871–7873.
[18] I. Srnova-Sloufova, F. Lednicky, A. Gemperle, J. Gemperlova, *Langmuir* **2000**, *16*, 9928–9935.
[19] E. Papaconstantinou, *Chem. Soc. Rev.* **1989**, *18*, 1–31.
[20] A. Troupis, A. Hiskia, E. Papaconstantinou, *Angew. Chem. Int. Ed.* **2002**, *41*, 1911–1914.
[21] S. Mandal, P. R. Selvakannan, R. Pasricha, M. Sastry, *J. Am. Chem. Soc.* **2003**, *125*, 8440–8441.
[22] S. Mandal, A. B. Mandale, M. Sastry, *J. Mater. Chem.* **2004**, *14*, 2868–2871.
[23] Y. R. Ma, L. M. Qi, W. Shen, J. M. Ma, *Langmuir* **2005**, *21*, 6161–6164.
[24] S. Link, Z. L. Wang, M. A. El-Sayed, *J. Phys. Chem. B* **1999**, *103*, 3529–3533.
[25] Ch. H. An, K. B. Tang, X. M. Liu, Y. T. Qian, *Eur. J. Inorg. Chem.* **2003**, 3250–3255.
[26] S. Zhang, H. L. Wang, Y. P. Bao, L. D. Zhang, *Life Sci.* **2004**, *75*, 237–244.
[27] A. Sanyal, S. Mandal, M. Sastry, *Adv. Funct. Mater.* **2005**, *15*, 273–280.
[28] C. S. Fadley, D. A. Shirley, *J. Res. Natl. Bur. Stand.* **1970**, *74 A*, 543.
[29] D. M. Chizhikov, V. P. Shchastlivyi, *Selenium and Selenides* (translated from Russian by E. M. Elkin), Collet's Ltd., London and Wellingborough, **1968**, p. 40.
[30] H. L. Zhu, R. S. Averback, *Philos. Magn. Lett.* **1996**, *73*, 27–33.
[31] M. Yeadon, M. Ghaly, J. C. Yang, R. S. Averback, J. M. Gibson, *Appl. Phys. Lett.* **1998**, *73*, 3208–3210.
[32] F. Banfield, S. A. Welch, H. Zhang, T. T. Ebert, R. L. Penn, *Science* **2000**, *289*, 751–754.
[33] A. P. Alivisatos, *Science* **2000**, *289*, 736–737.
[34] a) B. Mayers, K. Liu, D. Sunderland, Y. Xia, *Chem. Mater.* **2003**, *15*, 3852–3858; b) B. Gates, B. T. Mayers, A. Grossman, Y. Xia, *Adv. Mater.* **2002**, *14*, 1749–1752.
[35] Y. Xia, B. Gates, Y. Yin, Y. Lu, *Adv. Mater.* **2000**, *12*, 693–713.
Received: September 12, 2006
Published Online: February 2, 2007

 © 2007 Wiley-VCH Verlag GmbH & Co. KGaA, Weinheim